Research Article

The Effect of Ultrasonic Treatments on Current Transport Processes in Al-Al$_2$O$_3$-*p*-CdTe-Mo Structure

A. K. Uteniyazov [ID],[1] **A. Y. Leyderman** [ID],[2] **M. V. Gafurova** [ID],[3] **Kh. N. Juraev** [ID],[2] **and K. A. Dauletov** [ID][1]

[1]*Karakalpak State University, Ch. Abdirov Street 1, Nukus 230112, Uzbekistan*
[2]*Physical-Technical Institute, Scientific Association "Physics-Sun", Uzbek Academy of Sciences, Chingiz Aytmatov Street 2B, Tashkent 100084, Uzbekistan*
[3]*Academy of Science of Uzbekistan, Y. Gulomov Street 70, Tashkent 100047, Uzbekistan*

Correspondence should be addressed to A. K. Uteniyazov; abat-62@mail.ru

It was established that ultrasonic treatments (USTs) have practically no effect on the patterns of current flow in the Al-Al$_2$O$_3$-*p*-CdTe-Mo structure in the forward direction, namely, as in the absence of ultrasonic action, they appear in the sequence $J{\sim}V$, $J{\sim}V^2$, $J{\sim}V^{5.3}$, and J${\sim}V^2$. The effect of ultrasonic treatments affects only the magnitude of the flowing current; at low voltages, the current becomes somewhat larger, and at high voltages, it practically does not change. Changes in the magnitude of the flowing current are explained on the basis of the assumption that the recombination of nonequilibrium carriers in such a structure occurs through complex pair recombination complexes and, as a result of ultrasonic treatments, the number of both small acceptors and deep recombination centers increases.

1. Introduction

Currently, it is considered as an established fact that ultrasonic treatment (UST) affects structural defects and the electrophysical characteristics of semiconductors and semiconductor structures [1–8]. The advantages of UST compared with annealing and radiation exposure include the following features:

(1) The absorption of ultrasonic waves in a solid occurs predominantly in areas of disturbances of the periodicity of its crystal lattice and, therefore, the ultrasonic effect is more local

(2) The use of ultrasonic waves of different polarization and types allows to increase the selectivity of influence

(3) By selecting the frequency of ultrasonic vibrations, it is possible to achieve resonant transformations in the defective subsystem

It is known that the electrophysical and photoelectric properties of heterojunctions and MOS structures strongly depend on the properties of the surface of semiconductors. Since various surface effects directly affect the reliability and stability of virtually all types of semiconductor devices, the study of surface physics using metal-dielectric-semiconductor (MOS) structures plays a large role in all semiconductor technologies. The authors of Ref. [9, 10] investigated surface states at the interface of the Al-Al$_2$O$_3$-*p*-CdTe structure. In the Reference [11], it was shown that such a structure has the property of an injection photodetector and amplifies the primary photocurrent even in the absence of an external bias voltage. In the work [12], we investigated the effect of ultrasonic treatments on the electrophysical properties of the Al-Al$_2$O$_3$-*p*-CdTe structure. Ultrasonic treatments were carried out at the frequency of 2.5 MHz with the power of $P = 1$ W/cm^2 for 15 minutes. It was proved that UST significantly affects the fluctuations of surface charges at the interface and eliminates unstable point defects located in

the near-surface layer of a semiconductor. Experimental results have shown that the Al_2O_3 oxide layer formed between aluminum (Al) and cadmium telluride (CdTe) is of sufficient quality. It is proved that ultrasonic annealing of surface states in the upper half of the semiconductor bandgap at the interface of the Al-Al_2O_3-pCdTe-Mo structure leads to a decrease in the surface recombination current, and this, in turn, provides an increase in the number of electrons injected from the aluminum side into the base; therefore, the forward current increases after the UST. A decrease in the reverse current is due to the annealing of surface states in the lower half of the semiconductor bandgap, since this decreases the probability of tunneling of nonequilibrium electrons accumulated at the interface from the base into the metal. Experimental results have shown that the Al_2O_3 oxide layer formed between aluminum (Al) and cadmium telluride (CdTe) is of sufficient quality. Since the Al_2O_3 oxide layer is the main element in the studied Al-Al_2O_3-p-CdTe-Mo structure, a change in its properties, including the concentration of defects and impurities in the dielectric oxide layers (surface states) should affect the electrophysical and photoelectric properties of the entire structure. Therefore, this work is devoted to the study of the effect of ultrasonic treatments (UST) on the processes of current transport in the Al-Al_2O_3-p-CdTe-Mo-structure.

2. Experimental

Film structures p-CdTe from a columnar structure of grains on an Mo substrate are obtained by the sublimation methods in a hydrogen flow. It should be noted that when using hydrogen as a carrier gas, the transport of the vaporized substance is carried out at relatively lower temperatures than in the case of other inert gas compositions. In the synthesis of CdTe films in a flow of hydrogen H_2, the determining factor affecting their growth rate is the degree of excess of the metal components of cadmium vapor over the stoichiometric composition. This is explained by the fact that the components of Cd atoms are more volatile relative to Te atoms in CdTe vapor and is confirmed by the results of studies of the microstructure of the surface of the Al-p-CdTe-Mo structure on the surface of the CdTe film, as well as on the surface of aluminum. The elemental composition of the structure was studied using a JEOL JXA-8900R electron microprobe analyzer, using energy dispersive spectrometer (EMF) LINK ISIS (Japan). It was revealed that the atomic ratio of the components in the CdTe film is Cd/Te = 0.986 ≈ 1, which corresponds to the weak p-type conductivity of CdTe. Microcrystals of CdTe films grown at a substrate temperature $T_S = 670°C$ have high resistivity ($\rho = 10^9 \div 10^{11}$ Ω•cm) and have a mixed hexagonal and cubic structure. They have a columnar structure of grains in the direction of growth and were practically a single crystal. The cross-sectional grain sizes range from 100 to 150 μm. The thickness of the p-CdTe films was initially 40–50 μm, so that the grains penetrate the entire thickness of the film. The resulting films were brought to the required thickness (8–10 μm) by grinding

and polishing. Since at base thicknesses $d \leq 5 \mu$m, the Al-p-CdTe-Mo diode structure abruptly loses its rectifying properties. For example, the rectification coefficient, defined as the ratio of forward and reverse current at a fixed voltage (5 V), with a base thickness $d = 8$–10 μm is four to five orders of magnitude, and at $d \sim 5 \mu$m, it is only two orders of magnitude at the same value bias voltage. This is explained by the fact that the number of structural defects, including various complexes, inclusions, in the growing film at a distance of ~5 μm from the molybdenum substrate begins to increase sharply. The base thickness of the structure under study is $d \approx 10 \mu$m. In the course of sublimation in a stream of hydrogen, strongly compensated high-resistance large-block p-CdTe films of hole conductivity are synthesized. The p-CdTe films were synthesized from CdTe powders containing several impurities: copper, silver, and zinc. Therefore, strongly compensated high-resistance large-block p-CdTe films are probably formed.

The lifetime of minority charge carriers-electrons is $\tau \sim 10^{-8} \div 10^{-7}$ s. The value of τ_n was determined from the relaxation of nonequilibrium current carriers at a low level of excitation, both in the absence of voltage and at various applied voltages [13]. Nonequilibrium carriers were excited by an electric signal that was supplied from the calibrated pulse generator G5-55 of the V-shape with the amplitude 60–80 mV and the duration 100–200 μs. The steepness of such pulses was no more than $2 \cdot 10^{-9}$ s and duty cycle not less than $5 \cdot 10^{-4}$ s. The relaxation curve for the concentration of nonequilibrium variables at various stresses is described by an exponential dependence of the form as follows:

$$\Delta n = n_1 e^{-t/\tau}, \tag{1}$$

where t is the time and τ is the relaxation time constant. According to expression (1), value of the time constant was determined: $\tau_1 \approx 2 \cdot 10^{(-8)}$s in the absence of voltage and a $\tau_2 \approx 10^{-7}$ s at a constant voltage V = 1.2 V corresponding to the end section of a sharp increase in the current.

MOS structures were created on the surface of the films obtained by sputtering aluminum (Al) in vacuum (~10^{-5} Torr) [14]. In this case, the frontal aluminum contact had a thickness of ~$40 \div 50$ nm and an area of $S \approx 1$ cm^2. Here, the role of the rear electrical contact is played by the Mo substrate. The performed X-ray diffraction analysis showed [15, 16] that a thin Al_2O_3 oxide layer with a thickness of ~30 nm is formed in the technological process. This layer plays a very important role in the work of the obtained structure; it is thanks to it that it is not a simple metal-semiconductor structure that is obtained, but a MOS structure, i.e., Al-Al_2O_3-p-CdTe-Mo (Al metal, Al_2O_3, p-CdTe semiconductor, and Mo play the role of an ohmic contact). It is known that Al_2O_3 can be considered as a wide-gap n-type semiconductor. Thus, the obtained Al-Al_2O_3-p-CdTe-Mo structure can be represented as a R_{om}–n^+-p–R_{om} structure with a long p-base, the scheme of which is shown in Figure 1.
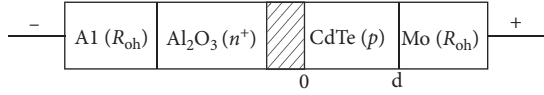
FIGURE 1: Scheme of Al-Al$_2$O$_3$-p-CdTe-Mo structure.

3. Results and Discussion

Figure 2 shows the dependences of the current-voltage characteristics of the structure in the forward and reverse branches before and after the UST on a double logarithmic scale.

The study shows that there is a power-law dependence of the current on the voltage of the.

Type $J = AV^{\alpha}$ and the exponents-α before and after the UST differ little. This means that the UST has practically no effect on the patterns of current flow in both forward and reverse directions. At the same time, experimental results show that UST leads to an increase in the current in the forward branch and to a decrease in the reverse branch of the I-V characteristic at the same bias voltage.

To establish the dependences of current transport, let us consider the current-voltage characteristics of the structure in the forward direction of the current before and after the UST (see Figure 3).

The study shows that there is a power-law dependence of the current on the voltage of the type $J = AV^{\alpha}$, and the exponent α before and after the UST practically does not differ. It can be seen from Figure 1 that both current-voltage characteristics have four parts, which are described by power-law dependences of the current on the bias voltage of the type $J \sim V^{\alpha}$ with different values of the exponent "α", namely, $J \sim V$, $J \sim V^2$, $J \sim V^{5.3}$, and $J \sim V^2$. In Ref. [17] such an I-V characteristics sequence was explained by a change in the conditions of recombination processes. Recombination processes occur first through simple local centers, then at high current densities, through complex complexes, inside which there is an exchange of nonequilibrium carriers. In particular, the linear region $J \sim V$ and the subsequent dependence $J \sim V^2$ are well explained in terms of the concept of recombination through simple local impurity centers. But then comes the part of the sharp increase of current $J \sim V^{\alpha}$, where $\alpha > 2$, and after that, it is the second quadratic part $J \sim V^2$, which does not fit into this model. Apparently, recombination processes occur through compound complexes.

Such compound complexes can be of various natures. They can initially be contained in a material, such as donor-acceptor pairs existing in A^2B^6 semiconductors or arise as a result of recombination-, temperature-, or photo-stimulated processes. The appearance of compound pair complexes is also possible as a result of radiation and other external influences. In Ref. [18], various models of such complexes were collected, and it was shown that the recombination statistics of nonequilibrium carriers, in this case, would differ from the classical Shockley–Read statistics. It can be donor-acceptor pairs, impurity + vacancy complexes, impurity + interstitial defect, or Frenkel pair type defects arising as a result of recombination-stimulated or photo-stimulated processes. In Ref. [18], various

models of such compound complexes are collected. In this case, the scheme of recombination occurring through such a two-level complex will be approximately the same for all models. It is shown in Figure 4. It is assumed that the difference $E_1 - E_2$ is very small, so you $e^{[(E_2 - E_1)/kT]}$ can ignore it. It was also shown in Ref. [18] that the rate of recombination occurring through all such complexes can be represented as

$$U = N \frac{c_{n1}c_{p2}(pn - n_i^2)}{c_{n1}(n + n_{11}) + c_{p2}(p + p_{12}) + \tau_i c_{n1}c_{p2}pn}, \quad (2)$$

where N is the concentration of complexes, c_{n1} is the coefficient of electron capture from the conduction band to the upper level E_1, c_{p2} is the coefficient of hole capture from the valence band to the lower level E_2, τ_i is the time of the intracomplex electron exchange, i.e., the electron exchange time between the levels E_1, and E_2, and n_{11} and p_{12} are analogues of the Shockley–Read statistical factors for levels E_1 and E_2, lying inside the bandgap and forming a pair recombination complex as follows:

$$n_{11} = N_c e^{-(E_c - E_1/kT)},$$
$$p_{12} = N_v e^{-(E_2 - E_v/kT)}. \quad (3)$$

In expression (2), the last term in the denominator describes the intracomplex electron exchange. When this member is small, i.e.,

$$c_{12}pn \ll c_{n1}(n + n_{11}) + (p + p_{12}), \quad (4)$$

then expression (2) is practically no different from the usual expression of the Shockley–Read statistics. In this case, the I-V characteristic for a sufficiently long diode (d/L >>1) is described by the well-known Lambert law as follows:

$$V = \sqrt{\frac{8d^3 J}{9q\mu_p\mu_n\tau_n N_A}} = B_0\sqrt{J}, \quad (5)$$

where μ_n is the electron mobility, τ_n is the electron lifetime, μ_p is the hole mobility, J is the current density, and d is the base thickness.

As already noted in Ref. [19], the Al-Al$_2$O$_3$-p-CdTe–Mo structure can be considered as an n^+-p structure with two ohmic metal contacts and a long base $d/Ln \sim 10$–20, where d is the length of the p base, i.e., the CdTe layer, and Ln is the diffusion length of minority carriers, i.e., electrons. By virtue of this, expression (5) well explains the first quadratic section.

As can be seen from Figure 1, the I-V characteristic at a low level of excitation, the dependence of current on voltage is described by a linear dependence and then a quadratic part appears.

Using the experimental results, we calculate the value of the product of mobility by the electron lifetime before the UST: $\mu_n\tau_n \approx 6.15 \times 10^{-6}$ cm^2/V. In this case, we first determine the value $B_0 \approx 95$ V cm A^{-1}, from the slope of the dependence $J \sim V^2$ (see Figure 1) and find the value $N_A \approx 10^{10}$ cm^{-3} from the linear
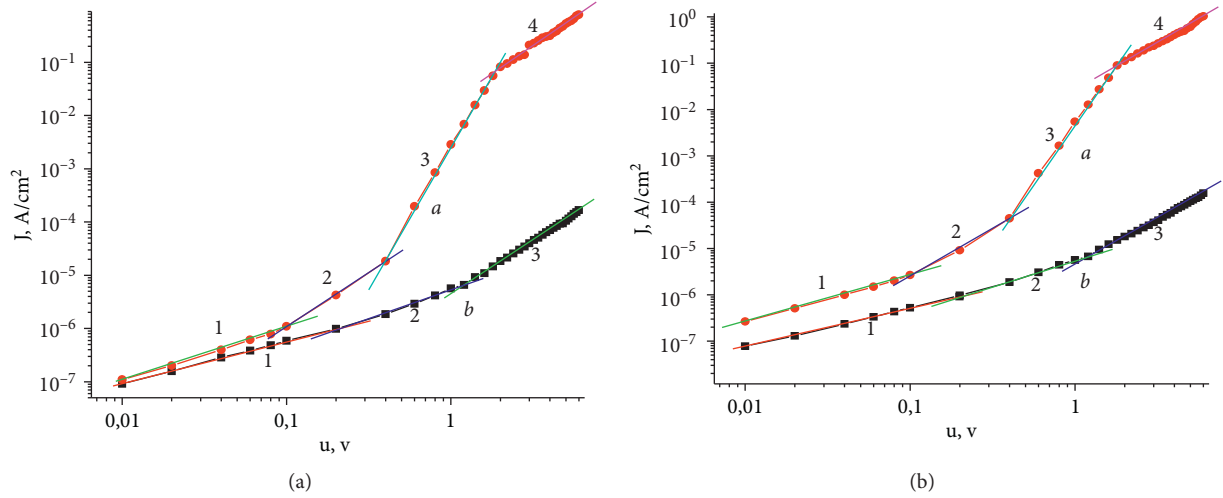
(a)

(b)

FIGURE 2: I-V characteristics of type I~V^α with different inclinations in the forward (a) and reverse (b) current directions up to I and after (II) UST. Ia: 1-1, 2-2, 3-5.3, 4-2; Ib: 1-0.84, 2-1, 3-2. IIa: 1-1, 2-2, 3-5, 4-2; IIb: 1-0.79, 2-1, 3-2.
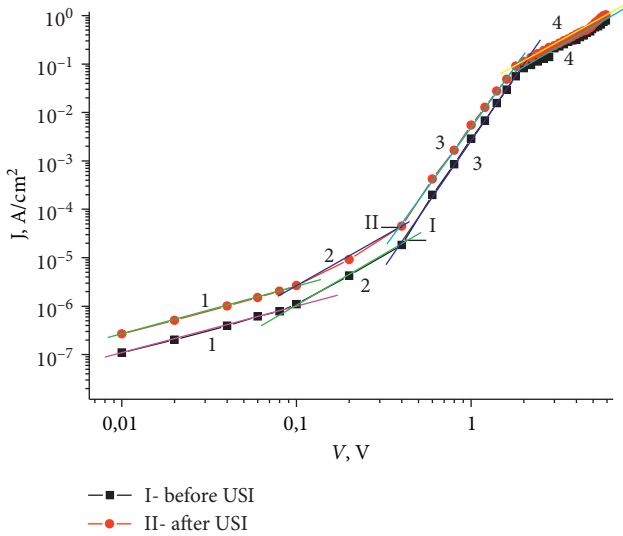

—■— I- before USI
—●— II- after USI

FIGURE 3: I-V characteristics of the type $J \sim V^\alpha$ with different slopes for the forward direction of the current before and after the UST. I 1-1, 2-2, 3-5.3, 4-2; II: 1-1, 2-2, 3-5, 4-2.
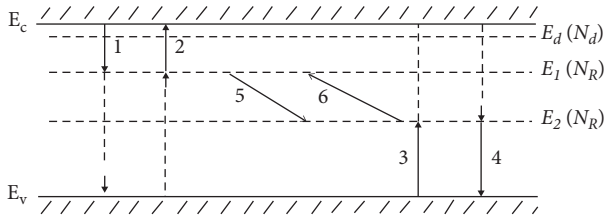

FIGURE 4: Recombination scheme through a pair recombination complex. Dashed lines show unaccounted transitions. $1 - c_{n1}N_R(1 - f_1)$; $2 - cn_1N_Rf_1n_{11}-$ level exchange E_1 with the conduction band. $3 - c_{p2}N_Rf_2p$; $4 - c_{p2}N_R(1 - f_2)p_{12}-$ level exchange E_2 with the valence band. $5 - c_{12}N_Rf_1(1 - f_2)$; $6 - c_{12}N_Rf_2(1 - f_1)e^{E_2 - E_1/kT}-$ exchange between levels E_1 and E_2 where $(c_{12})^{-1} = \tau_i-$ the time of intracomplex exchange.

part of the I-V characteristic. After UST, these parameters turned out to be equal: $\mu_n\tau_n \approx 5 \times 10^{-6}$ cm^2/V, $B_0 \approx 68$ V cm A^{-1}, and $N_A \approx 2.4 \cdot 10^{10}$ cm^{-3}. According to these data, the calculated values τ_n, at $\mu_n = 100$ cm^2/V s, turned out to be equal: $\tau_n \approx 6.15 \times 10^{-8}$ s and $\tau_n \approx 5 \times 10^{-8}$ s, respectively, before and after the UST. Such a constant time value almost coincides with published data [20]. Thus, the obtained experimental data indicate that, as a result of the action of USTs, the electron lifetime τ_n and the concentration of doping impurities N_A increase slightly, which well explains the small increase of current in the first quadratic part.

In Figure 1, after the quadratic part, there follows a section of a sharp increase of current, which is described by a power-law dependence of the type $J \sim V^\alpha$, where $\alpha > 2$. According to the theory [18], such part of a sharp increase of current is realized when the recombination of nonequilibrium current carriers occurs with a delay, i.e., involving complexes within which electronic exchange takes place. In this case, the I-V characteristic has the following analytical expression:

$$V = \frac{(b + 1)d^2N_R}{N_A\mu_n\tau_i} + \frac{d\sqrt{J}}{q\mu_n(b + 1)C} - \frac{2(b + 1)d^2N_R}{N_A\mu_nc_p\tau_iC\sqrt{J}} = A + B\sqrt{J} - \frac{D}{\sqrt{J}}.$$

(6)

In the structure under study, the base is a highly compensated semiconductor (p-CdTe); therefore, $N_A = N_a - N_d$ is the concentration of shallow acceptor centers, and the parameter C is related to the electron concentration by the ratio [18, 21] as follows:

$$n(0) = C\sqrt{J},$$

(7)

where $C = n_n/q(b + 1)V_p^*$, $V_p^* - V_p^*$ is the parameter due to the imperfection of the $n^+ - p$ junction.

From expression (6), one can determine such parameters as N_R/τ_i, $n(0)$, $c_n/a\tau_i$ (τ_i is the delay time inside the complex and N_R is the concentration of the complexes). Dependence (6) allows us to describe any value of the slope of the I-V

TABLE 1: Parameters determined from the I-V characteristics.

Samples	I-V characteristics part	$\mu_n\tau_n$, (cm^2•V^{-1})	N_R/τ_i, (cm^3•s^{-1})	n (0), (cm^{-3})	N_A, (cm^{-3})	$1/c_{p2}\tau_i$, cm^{-3}
Forward I-V						
1. Before UST	$J{\sim}V$ $J{\sim}V^2$ (Lampert's law) $J{\sim}V^{5.28}$ $J{\sim}V^2$	6.15•10^{-6}	5.6•10^{16} 2.45•10^{17}	2.26•10^{10}–5•10^{11} 2.95•10^{13}–9.1•10^{13}	10^{10}	1.02•10^{10}
2. After UST	$J{\sim}V$ $J{\sim}V^2$ (Lampert's law) $J{\sim}V^5$ $J{\sim}V^2$	5•10^{-6}	1.35•10^{17} 5.6•10^{17}	3.8•10^{10}–5.7•10^{11} 3.95•10^{13}–1.2•10^{14}	2.4•10^{10}	1.22•10^{10}

characteristic $J \sim V^\alpha$, including the part of the sharp increase. Composing a straight line equation for two given experimental points (J_1, V_1 and J_2, V_2), we determine the voltage value as follows:

$$V = V_1 - \frac{V_1 - V_2}{J_2 - J_1}J_1 \qquad (8)$$

which is equated to the value $A = (b+1)d^2N_R/N_A\mu_n\tau_i$ from formula (6); then using this expression, we determine the parameter N_R/τ_i. To determine the parameters, three experimental points (V_1, J_1), (V_2, J_2), and (V_3, J_3) were chosen from the part of the sharp increase of current, and for them, two equations were compiled to determine the coefficients B and D as follows:

$$B = \frac{V_2 - V_1}{\sqrt{J_2} - \sqrt{J_1}} - \frac{D\left(\left(1/\sqrt{J_1}\right) - \left(1/\sqrt{J_2}\right)\right)}{\sqrt{J_2} - \sqrt{J_1}},$$

$$D = \frac{(V_3 - V_2) - (V_2 - V_1)\sqrt{J_3} - \sqrt{J_2}/\sqrt{J_2} - \sqrt{J_1}}{\left(1/\sqrt{J_2} - 1/\sqrt{J_3}\right) - \left(1/\sqrt{J_1} - 1/\sqrt{J_2}\right)\sqrt{J_3} - \sqrt{J_2}/\sqrt{J_2} - \sqrt{J_1}}.$$

$$(9)$$

Then, equated them to the analytical values from formula (6). Next, substituting $d = 10\ \mu m$, $\mu_n = 100\ cm^2/V\,s$, and $N_A \approx 10^{10}\ cm^{-3}$ in these expressions, we determine the parameters: μ_nC, $1/c_{p2}\tau_i$. Then, using the formula (7), we determine the concentration of injected electrons $n(0)$ at the beginning and at the end of the third section. All parameters calculated from this part of the I-V characteristics are given in Table 1.

After the part of the sharp current increase, a quadratic part reappears. Such a sequence of I-V characteristics, according to the theory of [18], appears when the recombination rate through the complexes reaches full saturation $U \approx N_R/\tau_i$, in which case the quadratic I-V characteristic is described by the expression [18] as follows:

$$V = \frac{(b+1)d^2N_R}{2N_A\mu_n\tau_i} + \frac{d\sqrt{J}}{q\mu_n(b+1)}. \qquad (10)$$

The parameters determined from this site before and after USTs are, respectively, equal: $N_R/\tau_i \approx 2.45\times 10^{17}\ cm^{-3}$•s^{-1} and $N_R/\tau_i \approx 5.6 \times 10^{17}\ cm^{-3}$•s^{-1}, which are also listed in Table 1. The obtained N_R/τ_i values show that, at the same voltage value, the current in the second quadratic

part should practically not change, which confirms well the I-V characteristic as shown in Figure 1.

4. Conclusion

Thus, the experimental effect of UST on the structure Al-Al$_2$O$_3$-p-CdTe-Mo shows that, in the forward direction of the applied voltage, the current, as a result of the action of USTs, first increases slightly and then practically does not change. These facts clearly indicate that the physical nature of recombination processes changes as the current increases. At first, recombination processes take place under conditions when intracomplex exchange is insignificant, and the pair compound-complex behaves like a simple Shockley–Read trap. And then, at higher levels of injection, the role of intracomplex electron exchange increases, then parts of faster increase, and the second quadratic part appears. We would like to emphasize that these two parts, despite the external similarity, have a different physical nature. This is clearly seen from a comparison of formulas (4) and (10). In formula (10), we see the value of the time of intracomplex exchange, which is not in expression (4). This explains the different influence of USTs on the first and second quadratic parts. Apparently, the UST removes not only surface effects, as was noted in Ref. [12], but also volumetric ones, as a result of which the concentration of dopants and recombination complexes increases, which leads to an increase of current in the first quadratic part and changes it only a little in the second one.

In conclusion, we would like to emphasize that the study of the influence of USTs on current transport processes in the Al-Al$_2$O$_3$-p-CdTe-Mo structure unambiguously confirms the validity of the assumption that recombination processes in this structure occur through the compound pair recombination complex.

Data Availability

The data that support the findings of this research are available on request from the corresponding author (A.K. Uteniyazov).

Conflicts of Interest

The authors declare that they have no conflicts of interest.

Acknowledgments

References

[1] P. I. Baransky, A. E. Belyaev, S. M. Koshirenko et al., "The mechanism of change in the mobility of charge carriers in the ultrasonic treatment of semiconductor solid solutions," *Fizika Tverdogo Tela*, vol. 32, no. 7, p. 2159, 1990 in Russian.

[2] I. V. Ostrovskii, L. P. Stelbenko, and A. B. Nadtochii, "Ultrasound-induced surface hardening of dislocation-free silicon," *Semiconductors*, vol. 34, no. 3, pp. 251–254, 2000.

[3] E. B. Zaveryukhina, N. N. Zaveryukhina, L. N. Lezilova, B. N. Zaveryukhin, V. V. Volodarskii, and R. A. Muminov, "Acoustostimulated expansion of the short-wavelength sensitivity range of AlGaAs/GaAs solar cells," *Technical Physics Letters*, vol. 31, no. 1, pp. 27–32, 2005.

[4] O. Ya, "Features of dynamic acoustically induced modification of photovoltaic parameters of silicon solar cells," *Semiconductors*, vol. 45, pp. 798–804, 2011.

[5] A. Davletova and S. Zh. Karazhanov, "Open-circuit voltage decay transient in dislocation-engineered," *Journal of Physics D: Applied Physics*, vol. 41, no. 16, p. 165107, 2008.

[6] A. G. Pashayev, "Effect of various treatments on Schottky diode properties," *Semiconductors*, vol. 46, no. 8, pp. 1085–1087, 2012.

[7] I. B. Sapaev and Sh. A. Mirsagatov, "Influence of the ultrasonic irradiation on properties of the injection sensor based on pSi-nCdS-n$^+$CdS — structure and surface states density pSi-nCdS—heterojunction," *PSE*, vol. 12, no. 2, pp. 197–201, 2014.

[8] Sh. A. Mirsagatov, I. B. Sapaev, and Zh. T. Nazarov, "Ultrasonic annealing of surface states in the heterojunction of a p-Si/n-CdS/n$^+$-CdS injection photodiode," *Inorganic Materials*, vol. 51, no. 1, pp. 1–4, 2015.

[9] Sh. A. Mirsagatov and A. K. Uteniazov, "The surface states of the Schottky diode with the structureM (Al)-O (Al$_2$O$_3$)-S (CdTe)," in *Proceedings of the Solid State Physics. XIII International Science Conf*, pp. 100–103, Astana, Kazakhstan, 2016.

[10] Sh. A. Mirsagatov and A. K. Uteniazov, "The density of surface states at the interface of the structure M (Al)-O (Al$_2$O$_3$)-S (CdTe)," *Reports of the Academy of Sciences RUz*, vol. 5, pp. 18–22, 2016.

[11] A. K. Uteniazov and K. A. Ismaylov, "The spectral distribution of the photosensitivity of the structureM (Al)-O (Al$_2$O$_3$)-S (CdTe)," in *Proceedings of the Materials of the Republican scientific-practical conference with the participation of foreign scientists*, vol. 1, pp. 45–48, Nukus, Uzbekistan, 2018.

[12] A. K. Uteniyazov and K. A. Ismailov, "Effect of ultrasound irradiation on the electrophysical properties of the structure of Al–Al$_2$O$_3$–CdTe," *Semiconductor Physics, Quantum Electronics & Optoelectronics*, vol. 22, no. 2, pp. 165–170, 2019.

[13] S. A. Mirsagatov, A. K. Uteniyazov, and A. S. Achilov, "Mechanism of current transport in Schottky barrier diodes based on coarse-grained CdTe films," *Physics of the Solid State*, vol. 54, no. 9, pp. 1751–1763, 2012.

[14] S. A. Mirsagatov and A. K. Uteniyazov, "Injection photodiode based on p-CdTe film," *Technical Physics Letters*, vol. 38, no. 1, pp. 34–37, 2012.

[15] Sh. A. Mirsagatov, S. A. Muzafarova, M. S. Baiyev, and A. S. Achilov, "The study of real structures of a diode with a Schottky barrier Al-p-CdTe," *Uzbek Journal of Physics*, vol. 12, pp. 154–160, 2010.

[16] A. S. Achilov, B. N. Zaveryukhin, M. U. Kalanov, and V. M. Rustamova, "X-ray studies structures of a new type of A$_2$B$_6$ receiver of electromagnetic radiation," *Reports of the Academy of Sciences RUz*, vol. 2, pp. 24–26, 2014.

[17] Sh. A. Mirsagatov and A. K. Uteniyazov, "The mechanism of current transport in the structure Al-p-CdTe-Mo with different thickness of the base"" *PSE*, vol. 13, no. 3, pp. 325–329, 2015.

[18] A. Y. Leyderman and M. K. Minbaeva, "Mechanism of rapid growth of the direct current in semiconductor diode structures," *Semiconductors*, vol. 30, no. 11, pp. 1729–1738, 1996.

[19] A. Y. Leyderman, A. K. Uteniyazov, and M. T. Nsanbaev, "Recombination processes in the Al-n-Al$_2$O$_3$-p-CdTe-Mo structure," in *Proceedings of the International Scientific journal "Global science and innovations 2020: Central Asia*, vol. 3, no. 3, pp. 29–32, Nur-Sultan, Kazakhstan, February 2020.

[20] M. A. Lampert and P. Mark, *Current Injection in Solids*, Academic Press, Cambridge, England, 1970.

[21] E. I. Adirovich, P. M. Karageorgiy-Alkalaev, and A. Y. Leyderman, *Double Injection Currents in Semiconductors*, p. 320, Sovetskoe Radio, Moscow, Russia, 1978.